Flow Measurement and Instrumentation 54 (2017) 136–145

Contents lists available at ScienceDirect

Flow Measurement and Instrumentation

journal homepage: www.elsevier.com/locate/flowmeasinst

Unsteady velocity profiling in bores and positive surges

Xinqian Leng[a], Hubert Chanson[a,*]

[a] The University of Queensland, School of Civil Engineering, Brisbane QLD 4072, Australia

ARTICLE INFO

Keywords:
Positive surge
Unsteady velocity profiling
Instantaneous velocity
Ensemble average
Open channel flows
Physical modelling

ABSTRACT

In an open channel, steady flow conditions may be achieved when the discharge and boundary conditions remain constant for a reasonable period of time. The operation of any regulation device (e.g. gate) is associated with some unsteady surge motion. In the present study, new velocity profiling measurements were performed systematically under controlled flow conditions. Both steady and unsteady measurements were conducted in a relatively large laboratory facility. An ensemble-averaged technique was applied in unsteady flows to investigate positive surges. The experiments were repeated 25 (or 50) times for each controlled flow condition and the results were ensemble-averaged. The quality and accuracy of the Profiler data set were validated against data collected with an acoustic Doppler velocimeter, in both steady and unsteady rapidly-varied flows. A careful sensitivity analysis was conducted to test the appropriate number of runs. The results indicated that the selection of 25 runs was suitable for ensemble-averaging in rapidly-varied unsteady flows. Some instrumental error was observed however with the velocity profiler. Outside the boundary layer, the Profiler tended to produce errors in terms time-averaged velocity data and velocity fluctuations for a number of points in a profile. Overall, the study demonstrated that the propagation of positive surges is a highly unsteady turbulent process, and the performance of ADV Vectrino II Profiler in such an unsteady turbulent flow was satisfactory, provided that a careful validation was undertaken for all Profiler outputs.

1. Introduction

In an open channel, steady flow conditions may be achieved when the discharge and boundary conditions remain constant for a reasonable period of time. The operation of any regulation device such as a gate is associated with some unsteady surge motion propagating upstream and downstream of the device [17,3]. A positive surge or bore is the unsteady flow motion characterised by a sudden increase in water depth [14,17]. It is also called compressive wave or hydraulic jump in translation [11,18]. Fig. 1 presents a positive surge propagating in a rectangular channel. Geophysical applications include tidal bores and tsunami propagating into river systems. Turbulence in open channel flows has been studied for decades [21–23,28]. Most data were obtained in steady flows: e.g., using laser Doppler anemometry, particle image velocimetry, acoustic Doppler velocimetry. Measurements in rapidly-varied unsteady open channel flows are less common [12,13].

In a hydrodynamic shock like a positive surge, experiments must be repeated systematically to derive turbulence properties based upon ensemble-averaging [6]. The process is repetitive and time-consuming, and it could be potentially shortened using a fast response profiling system, such as a Nortek™ acoustic Doppler velocimeter Vectrino II Profiler. Introduced in 2010–2011, the validation literature of the Vectrino II Profiler remains limited albeit revealing [8],[19]. A numbers of issues were reported, including: "*there appear to be small systematic errors in the probe calibration, particularly in the cells closest to the transmitter*" [8]; "*failure of the two overlapping Vectrino II profiles of Reynolds stress to coincide*" [30]; "*turbulence [measurement] appears to be highly sensitive to the distance from the transducer, particularly for the lateral and streamwise components*" [19]; "*signal noise in the 1–10 Hz range results in poor estimates of higher order statistical moments above* and "*some measurement nodes close to the boundary exhibit random noise*" [9].

In the present study, new velocity profiling measurements were performed systematically under carefully controlled flow conditions. Both steady and unsteady measurements were conducted in a relatively large laboratory facility. An ensemble-averaged technique was applied to unsteady flows to investigate positive surges. All experiments were repeated 25 (or 50) times for each controlled flow condition and the results were ensemble-averaged. The quality and accuracy of the Profiler data set were validated against data collected with an acoustic Doppler velocimeter, in both steady and unsteady rapidly-varied flows.

* Corresponding author.
E-mail address: h.chanson@uq.edu.au (H. Chanson).

http://dx.doi.org/10.1016/j.flowmeasinst.2017.01.004
Received 13 May 2016; Received in revised form 21 December 2016; Accepted 7 January 2017
Available online 09 January 2017
0955-5986/

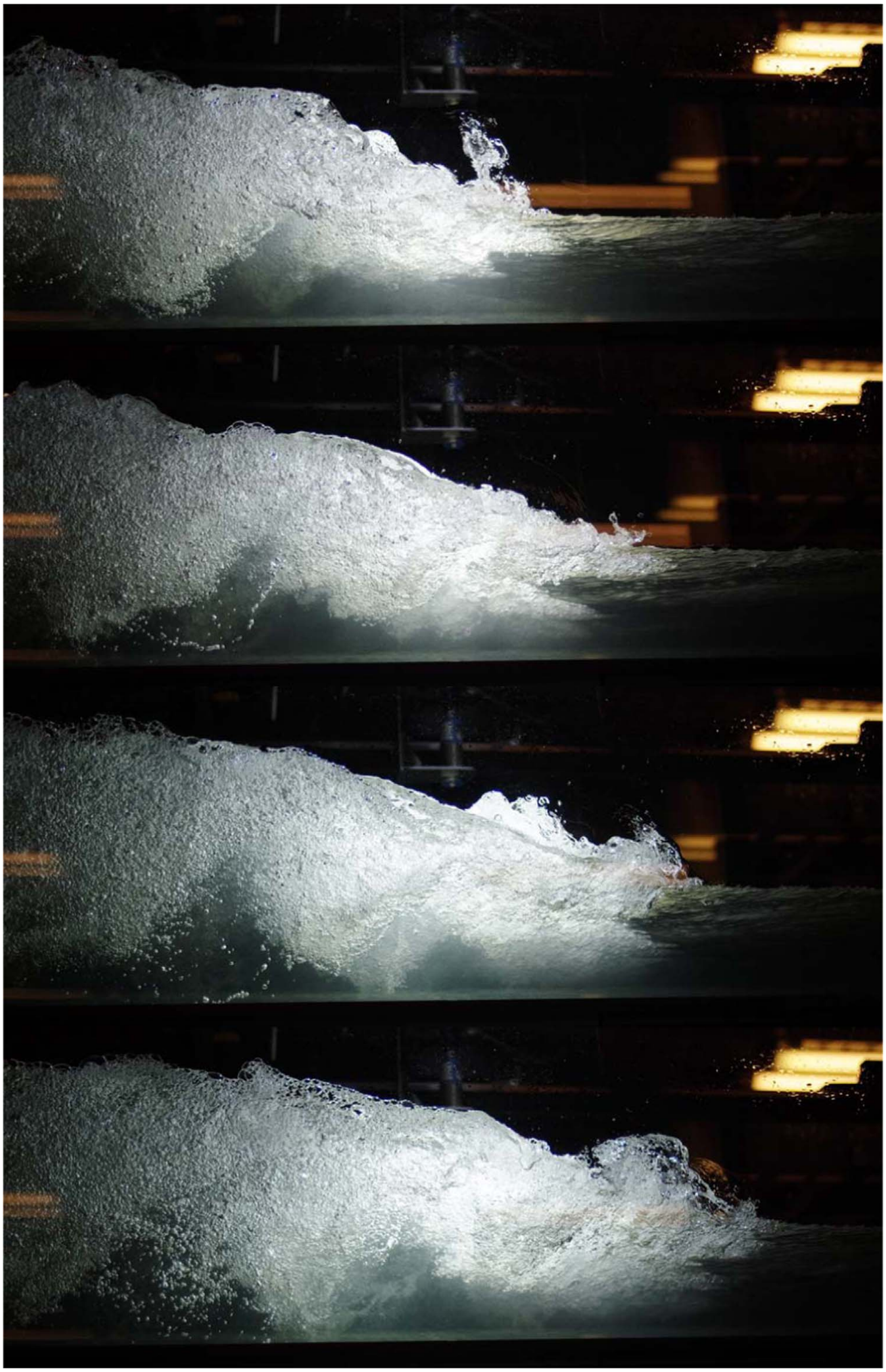

Fig. 1. Positive surge propagating upstream - Initial flow: Q =0.102 m^3/s, surge Froude number: Fr_1 =2.2, bore propagation from left to right, 120 ms between shots (from top to bottom), shutter speed 1/4,000 s.

2. Instrumentation, experimental setup and flow conditions

2.1. Velocity measurements

Three velocimetry systems were considered in the present study: a Nortek™ acoustic Doppler velocimeter Vectrino II Profiler (Serial number P27338, Hardware ID VNO 1366), a Nortek™ acoustic Doppler velocimeter (ADV) Vectrino+(Hardware ID VNO 0436), and Prandtl Pitot tubes.

The Vectrino II Profiler, referred to as Profiler, is a high-resolution acoustic Doppler velocimeter used to measure turbulence and three-dimensional water velocity [24]. The basic measurement technology is coherent Doppler processing [24,30]. Herein the Profiler (firmware v. 1950) was equipped with a fixed downward-looking head (hardware ID VNO1366), one central emitter and four receivers. The Profiler software version was 1.22. (Note that the physical experiments were conducted in 2015, prior to the introduction of any manufacturer's re-calibration and of probe upgrade, both introduced in 2016.) The

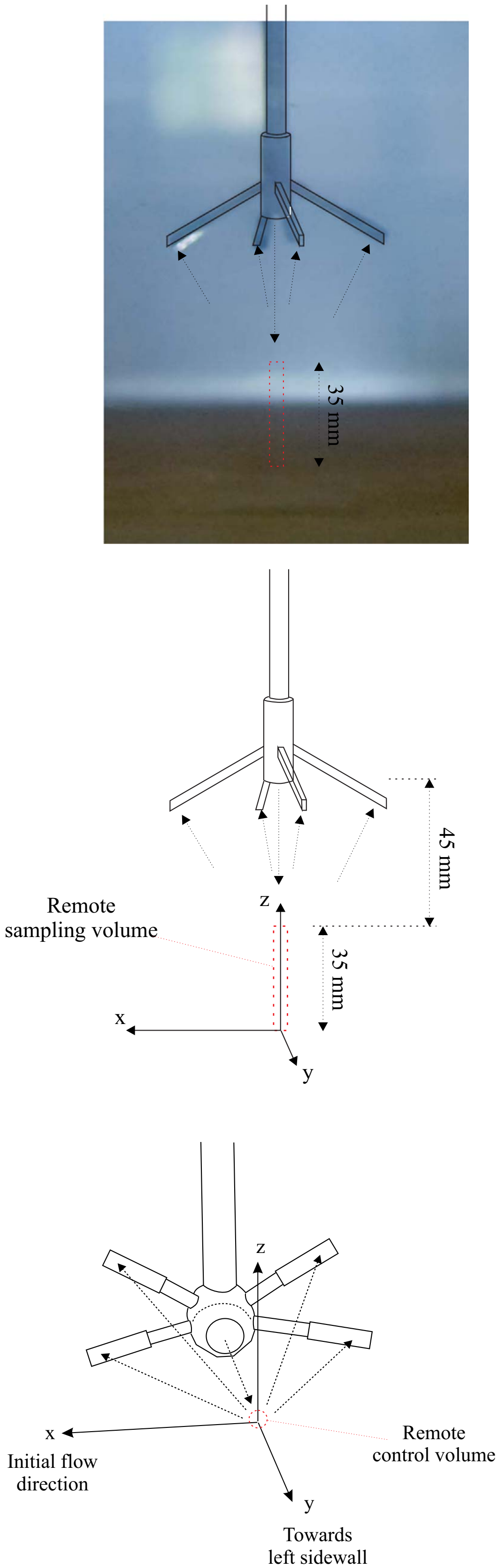

Fig. 2. Coordinated sketches of ADV Vectrino II Profiler and ADV Vectrino+.

Profiler was capable of recording velocity components quasi-simultaneously in a vertical profile of up to 35 mm in height (Figs. 2A and 3C). The minimum distance from the emitter was 40 mm to the first point of the profile. Two profiling ranges were tested: 30 and 35 mm. The height of each sampling cell was 1 mm: e.g., a profiling range of 35 mm consisted of 35 sampling cells sampled simultaneously. The velocity range was ± 1.0 m/s and the sampling frequency was 100 Hz herein. The Profiler was located at x=2.0, 7.87 m or 8.5 m, where x was the longitudinal distance measured from the channel upstream end (Fig. 3A) (see next section).

The Vectrino+ unit, referred to as ADV, was used to validate the Profiler data in steady and unsteady flows. The ADV was equipped with a three-dimensional side-looking head (Fig. 2B). The ADV was set up with a velocity range ± 1.0 m/s, a transmit length of 0.3 mm, a sampling volume of 1.5 mm height and power setting High. Two sampling frequencies were used. For the steady flow measurements, the ADV was sampled at 200 Hz. During the unsteady flow experiments, the ADV was sampled at 100 Hz.

The Prandtl-Pitot tubes were used to validate the ADV velocity data in steady flows. One tube was a Dwyer® 166 Series Prandtl-Pitot tube with a 3.18 mm diameter tube made of corrosion resistant stainless steel, and featured a hemispherical total pressure tapping (Ø =1.19 mm) at the tip with four equally spaced static pressure tappings (Ø =0.51 mm) located 25.4 mm behind the tip. The tip design met AMCA and ASHRAE specifications and the tube did not require calibration. The other Prandtl-Pitot tube had an external diameter of 3.05 mm. The total pressure was measured through a 1.2 mm diameter tapping and the piezometric pressure was recorded with eight 0.5 mm diameter holes spaced around the tube circumference. The dynamic and static tappings were separated 24.5 mm.

The Profiler output data were post-processed with the Matlab program VTMT version 1.1 [1]. while the ADV signal was post-processed with the software WinADV 2.030. In steady flows, the post-processing included the removal of data with average correlation values less than 90% and average signal to noise ratio less than 5 dB. In addition, the phase-space thresholding technique developed by Goring and Nikora [10] was applied to remove spurious points in the data set. In the unsteady flows, the above post-processing technique was not applicable (Nikora 2004, Person. Comm., [4,13]), and raw data was used directly for analysis.

2.2. Experimental facility

The experimental channel was 19 m long and 0.7 m wide, made of glass side walls and smooth PVC horizontal bed. The initially steady flow was supplied by the upstream water tank leading to the glass-sidewall test section through a series of flow straighteners followed a smooth three-dimensional convergent intake. The discharge provided by the tank was measured with a magneto-flowmeter with an accuracy of 10^5 m^3/s; it was checked systematically against the brink depth d_b at the flume's downstream end (x=19 m). A fast-closing Tainter gate was located next to the channel's downstream end at x=18.1 m. The positive surge was generated by the rapid Tainter gate closure and the surge propagated upstream as sketched in Fig. 3A. A radial gate was located at x=18.88 m to control the initial water elevation. Unsteady free-surface measurements were performed using a series of acoustic displacements meters (ADMs) located at various positions x=18.17 m, 8.5 m and 7.93 m. All ADMs were calibrated against point gauge measurements in steady flows, and sampled at 200 Hz on the channel centerline. The ADMs were synchronised with the ADV and Profiler within 1 ms.

First steady flow velocity measurements were performed using the Profiler over a wide range of flow conditions, listed in Table 1. The Profiler data were compared systematically to ADV measurements sampled simultaneously. Both ADV and Profiler were located at x=7.87 m. The Profiling range was 30 mm, and the ADV control volume was located at the centre of the Profiling range. Fig. 3 presents an overview of the experimental channel and instrumental setup.

Second unsteady ensemble-averaged velocity measurements were

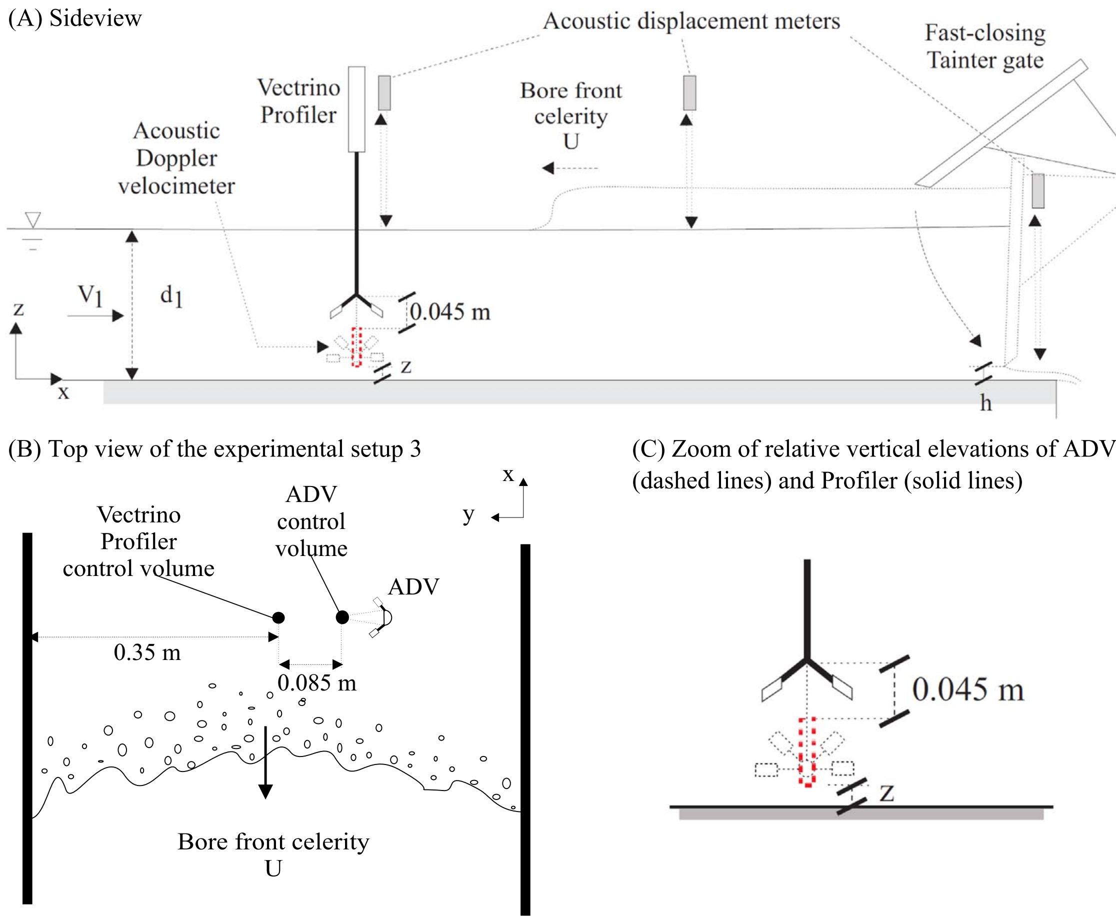

Fig. 3. Sketches of the experimental channel and instrument setup 3 - Thick black line indicates channel side walls) during the preliminary velocity measurements. (A) Sideview. (B) Top view of the experimental setup 3. (C) Zoom of relative vertical elevations of ADV (dashed lines) and Profiler (solid lines).

performed using the Profiler, and the results were validated against ADV data (Table 1). In the unsteady flow, the experiments were repeated 50 times to obtain the ensemble-averaged velocity properties. A sensitivity analysis was performed to find the appropriate number of repeats to characterise accurately the rapidly-fluctuating velocity characteristics (Section 4.3). Two instrumental setups were used during the ensemble-averaged measurements to minimise instrument interferences between Profiler and ADV (Fig. 4). In Setup 1, the Profiler was sampled alone at x=8.5 m, with a profiling range of 35 mm. In Setup 2, the Profiler was located at x=8.5 m, sampled simultaneously with an ADV located 0.57 m upstream. The control volume of the ADV was placed at the bottom of the profiling range.

2.3. Experimental flow conditions

Preliminary tests were conducted to compare the ADV and Prandtl-Pitot tube data in steady flows [27,29]. The results showed a close agreement between Pitot and ADV velocity measurements within 2%. Further the velocity distributions were integrated across the channel width to check for conservation of mass:

$$Q = \int_{y=0}^{B} \int_{z=0}^{d} V_x \times dz \times dy \tag{1}$$

where V_x is the longitudinal velocity component, y and z are respectively the transverse and vertical coordinates, d is the water depth and B is the channel width. The results showed a close agreement within 2% between Eq. (1) and the measured discharge, which was measured

Table 1
Experimental flow conditions for steady flow and positive surge experiments.

Q (m^3/s)	d_1 (m)	x (m)	Fr_o	Fr_1	Radial gate opening (m)	h (m)	z/d_1	Instrumentation	Remark
0.100	0.177	2.00 7.87 8.50	0.60	1.58	N/A	0	0.00–0.73	ADV & Profiler	Steady flow & ensemble-averaged unsteady velocity measurements
0.085	0.161	7.87	0.60	–	N/A	N/A	0.00–0.60	ADV & Profiler	Steady flow
0.071	0.144	7.87	0.59	–	N/A	N/A	0.00–0.63	ADV & Profiler	Steady flow
0.100	0.215	7.87	0.45	–	0.112	N/A	0.00–0.70	ADV & Profiler	Steady flow
0.086	0.211	7.87	0.40	–	0.090	N/A	0.00–0.71	ADV & Profiler	Steady flow
0.071	0.21	7.87	0.33	–	0.670	N/A	0.00–0.71	ADV & Profiler	Steady flow
0.055	0.201	2.00	0.27	–	0.05	N/A	0.00–0.75	ADV & Profiler	Steady flow

Notes: d_1: initial flow depth; Fr_o: initial steady flow Froude number; Fr_1: positive surge Froude number; N/A: denotes that the radial gate was fully opened; Q: water discharge; h: Tainter gate opening after closure; x: longitudinal Profiler location; z: vertical elevation above bed.

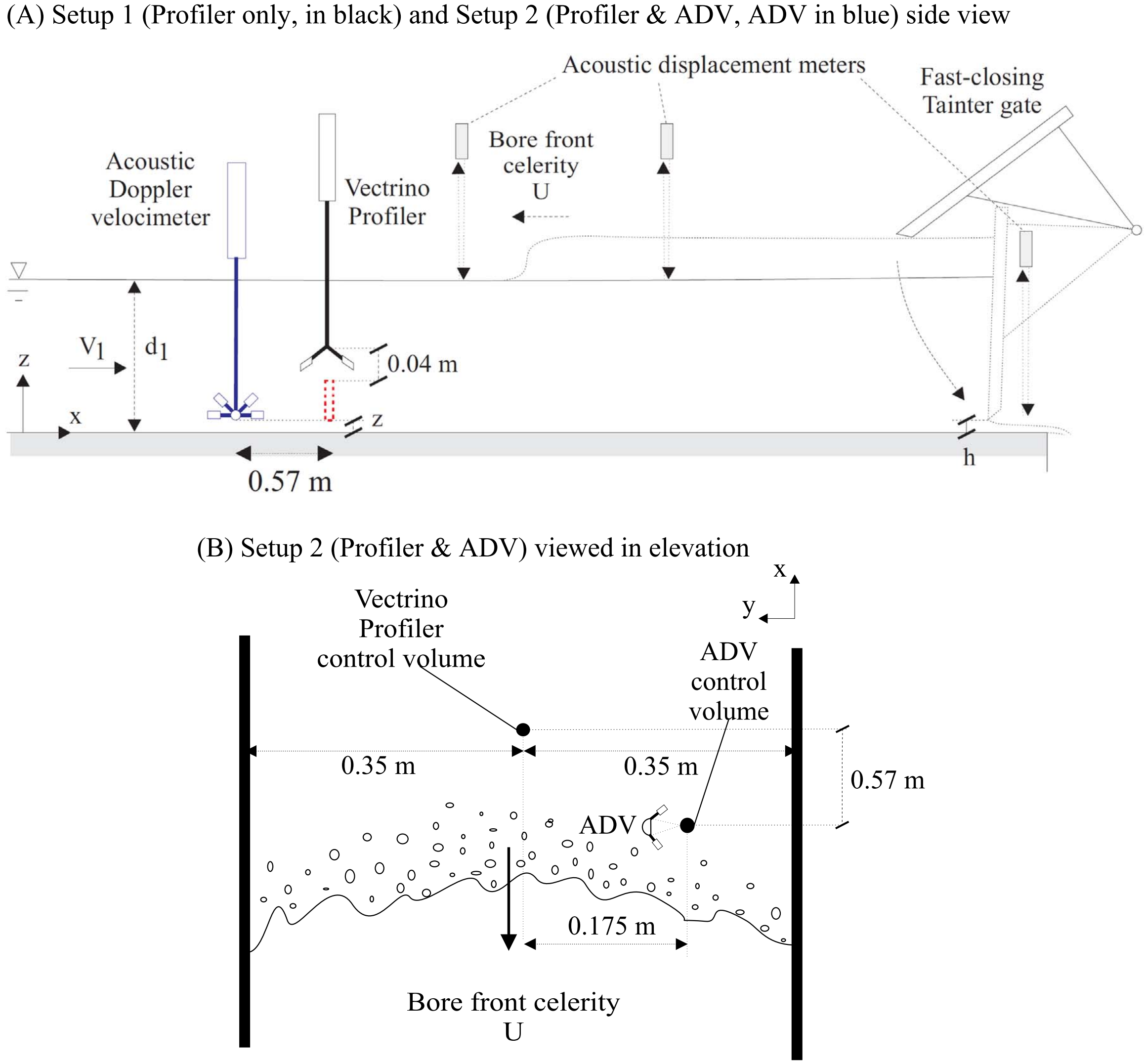

Fig. 4. Experimental channel and instrument setup for the ensemble-averaged measurements. (A) Setup 1 (Profiler only, in black) and Setup 2 (Profiler & ADV, ADV in blue) side view. (B) Setup 2 (Profiler & ADV) viewed in elevation.

independently with a flow meter installed on the water supply line.

The experimental flow conditions are summarised in Table 1, where d_1 is the initial steady flow depth at the velocity sampling location, Fr_o and Fr_1 are the Froude numbers for the initially steady flow and of the positive surge respectively, h is the Tainter gate opening after closure, and z/d_1 is the dimensionless vertical elevation, with z the sampling volume elevation above the invert. The radial gate opening height is denoted N/A when it was fully opened. Table 2 lists the different setups used to test several combinations of Profiler and ADV. Figs. 3 and 4 present sketches showing three configurations. In the present study, Brisbane tap water was used and no seeding was applied. Further details were reported by Leng and Chanson [15].

3. Steady flow measurements using Vectrino II Profiler

3.1. Steady flow velocity measurements

For all flow conditions, steady flow velocity measurements showed a close agreement between Profiler and ADV data in terms of time-averaged velocity components. The finding was generally consistent with the earlier findings of [8], [30], and [19]. However outlier points occurred slightly above the outer edge of the boundary layer. This is illustrated in Fig. 5 showing typical vertical profiles of time-averaged longitudinal velocity V_x and velocity fluctuations at two longitudinal locations: x=2.0 m and 7.87 m, where the relative boundary layer thickness was δ/d_1 =0.09 and 0.42 respectively. The occurrence of

Table 2
Instrumentation configurations.

Setup	Instrumentation	Profiler location	ADV location	Remarks
1	Profiler only	x = 8.5 m, y = 0.35 m	N/A	
2	Profiler and ADV	x = 8.5 m, y = 0.35 m	x = 7.93 m, y = 0.225 m	ADV emitter facing right sidewall
3	Profiler and ADV	x = 8.5 m, y = 0.35 m	x = 8.5 m, y = 0.215 m	ADV emitter facing right sidewall
4	Profiler and ADV	x = 8.5 m, y = 0.35 m	x = 7.93 m, y = 0.225 m	ADV emitter facing Profiler
5	ADV only	N/A	x = 8.5 m, y = 0.35 m	

Notes: x: longitudinal location; y: transverse distance measured from the right sidewall.

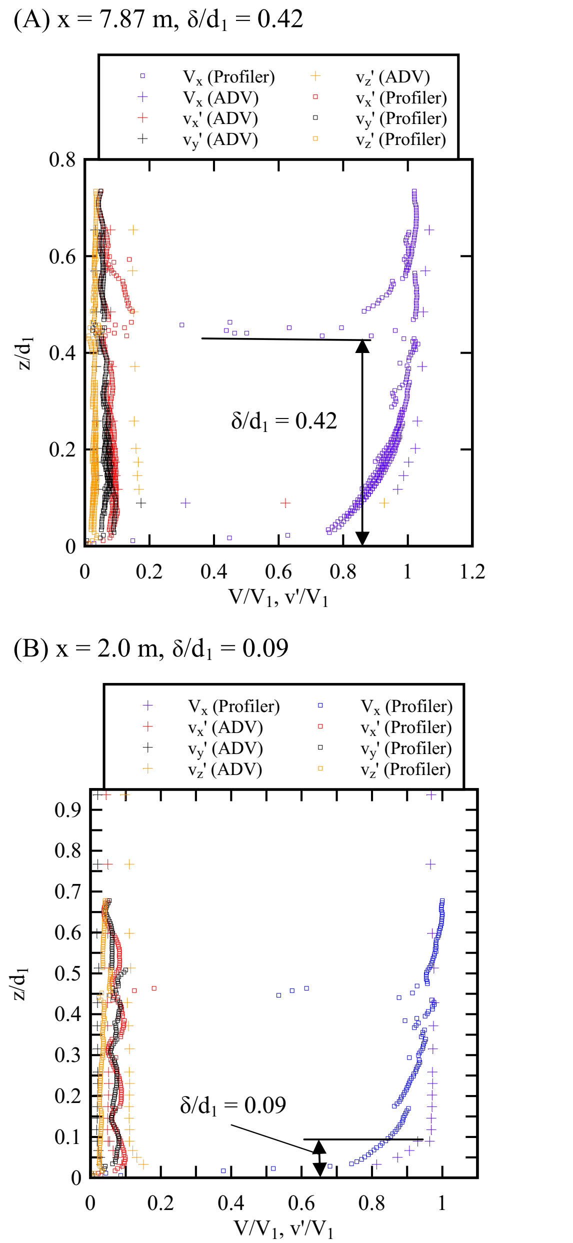

Fig. 5. Vertical profile of the time-averaged longitudinal velocity and velocity fluctuations in steady flow: comparison between ADV and Profiler data - Q =0.100 m^3/s, d_1 =0.177 m,Re =1.5×10^5. (A) x=7.87 m, δ/d_1 =0.42. (B) x=2.0 m, δ/d_1 =0.09.

suspicious points was consistent for all velocity components: when the longitudinal velocity showed outlying data at particular vertical elevations, similar outliers would be observed at the same vertical elevations with the other velocity components.

In the wall region of steady developing boundary layer flow, the vertical distribution of the time-averaged longitudinal velocity V_x follows a logarithmic velocity law, also called the log law or law of wall [25,26]. For a smooth turbulent boundary layer, the log law gives:

$$\frac{V_x}{V_*} = \frac{1}{\kappa}\times \mathrm{Ln}\left(\rho\times\frac{V_*\times z}{\mu}\right)+D_1 \quad 30 \text{ to } 70 < \rho\times\frac{V_*\times z}{\mu} \text{ and } \frac{z}{\delta} < 0.1 \text{ to } 0.2 \qquad (2)$$

where V_* is the shear velocity: $V_*= (\tau_o/\rho)^{1/2}$, κ is the von Karman constant (κ=0.4), τ_o is the boundary shear stress, z is the vertical elevation from the surface of the channel bed, ρ and μ are the fluid density and dynamic viscosity respectively, D_1 is an integration constant equal to 5 [26,5].

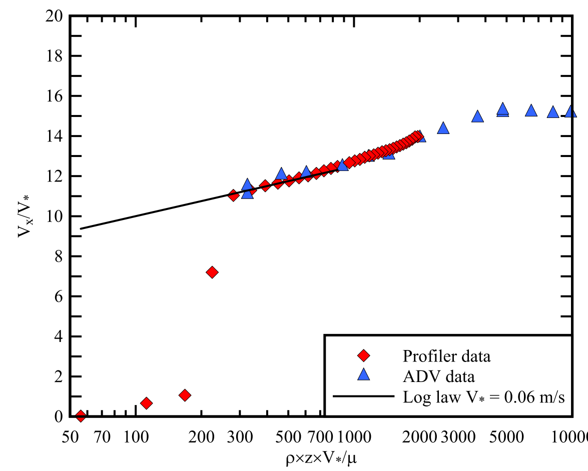

Fig. 6. Logarithmic velocity profiles in the initially-steady flow at x =8.5 m for Q =0.099 m^3/s and d_1 =0.171 m - Comparison between Profiler data (red symbols), ADV data (blue symbols) and theoretical log law (black line).

Present longitudinal velocity data within the inner region of the boundary layer ($z/\delta < 0.1$ to 0.2) were compared to the theoretical log law profile. Fig. 6 presents a typical example; the Profiler data are compared to ADV measurements and the log law within the wall region. Note that the shear velocity was estimated using the best fit of the log law. Overall, the majority of wall region data points followed the theoretical log law curve, except for the first four to five data points, corresponding to locations less than 6 mm from the bed. The Profiler measurements compared well with the ADV measurements further above (Fig. 6). Note that, in the close vicinity of the bed ($z/\delta < 0.1$), no ADV data was available due to physical limitation (i.e. side-looking head design).

The boundary shear stress τ_o was estimated using several methods. Herein, τ_o was deduced from the best fit of the log law, and compared to the tangential Reynolds stress $\rho\times v_x\times v_z$ in the vicinity of the bed. Further the average shear stress was calculated based upon the measured longitudinal free-surface profile and discharge. The results are summarised in Table 3 in terms of the dimensionless boundary shear stress (i.e. Darcy-Weisbach friction factor). All methods yielded dimensionless boundary shear stresses of the same order of magnitude, ranging from 0.02 to 0.06. Note that the boundary friction deduced from the tangential Reynolds stress data was considered the least accurate, due to some effect of bubbles entrained in the wake of the intruding Profiler stem.

Over the entire developing boundary layer, the Profiler and ADV data compared well in terms of longitudinal velocity component. The velocity profiles followed closely a 1/N power law, with N ranging from 8 to 11. Assuming such a power law in the boundary layer, the free-stream velocity data V_{max} data (Table 3) were checked against the

Table 3
Free-stream velocity, shear velocity and dimensionless boundary shear stress (Darcy-Weisbach friction factor) in the initially steady flow.

Q	d_1	V_1	Fr_o	V_{max}	Log	law	Backwater	$\rho\times v_x\times v_z$
					V_*	f_1	f_2	f_3
(m^3/s)	(m)	(m/s)		(m/s)	(m/s)			
0.099	0.197	0.72	0.52	0.77	0.06	0.06	0.04	0.04
0.099	0.171	0.83	0.64	0.88	0.06	0.04	0.02	0.03
0.099	0.097	1.46	1.50	1.58	0.11	0.05	0.02	–

Notes: Fr_o: steady flow Froude number; V_{max}: free-stream velocity in steady flow; V_*: shear velocity deduced from best fit of log law; f_1: dimensionless boundary shear stress deduced from best fit of log law: $f_1 = 8\times V_*^2/V_1^2$; f_2: dimensionless boundary shear stress deduced from best fit of backwater profile to the steady flow free-surface data; f_3: dimensionless boundary shear stress deduced from the tangential Reynolds stress $\rho\times v_x\times v_z$ in steady flows near bed.

equation of conservation of mass:

$$\frac{Q}{B} = \left(\left(\frac{N}{N+1} - 1\right) \times \frac{\delta}{d_1} + 1\right) \times V_{max} \times d_1 \qquad (3)$$

where B is the channel width and N is derived from the best fit of power law. Eq. (3) compared well to the measured specific discharge within 10% for all flow conditions. Outside of the boundary layer, the theoretical velocity distribution was a straight line: $V_x = V_{max}$. Although the ADV data showed a close match to the theoretical estimate, the ADV Profiler data deviated slightly from the ADV and theoretical results, mostly at the top and bottom cells of each profile as observed by [19].

The velocity fluctuations were characterised by the standard deviation of velocity data v′. Fig. 5 highlights some inconsistent vertical pattern in terms of velocity fluctuation data throughout the water column, especially with a thin boundary layer (Fig. 5B). [19,30] also showed errors in velocity variance using the same profiling instrument. Larger differences were observed in terms of vertical velocity fluctuations, compared to other velocity components. This could be some effect of the bed proximity on the receiver for the vertical velocity component, as previously observed with ADVs [20,7]. The experiments were conducted at two longitudinal locations x=2.0 m and 7.87 m to examine the occurrence of error points in relation to the boundary layer thickness. The results suggested no obvious difference, in terms of both locations and quantity. However, the number of error points was significantly larger with measurements conducted with the smaller discharge (Q =0.055 m^3/s) at both longitudinal locations.

Overall the steady flow velocity measurements highlighted a number of advantages and issues with the Profiler. The Profiler was reliable for the measurements of vertical profile of time-averaged longitudinal, transverse and vertical directions in a turbulent flow with high temporal resolution (100 Hz), together with the ability to simultaneously sample velocity characteristics at up to 35 closely-spaced locations. Error points existed in the sampling profile for which the recorded velocity values were not meaningful. The error points were typically located outside the outer edge of the boundary layer. Although their occurrences seemed to be random and discontinuous, their geometrical locations in a single profile were consistent (i.e. at same fixed vertical elevation) for a given flow condition and could be reproduced by repeating the experiment. Therefore such locations are relatively easy to avoid. The presence of error points ('weak spots') in the Profiler measurements was related to flow discharge and vertical elevation rather than turbulent flow properties.

3.2. Discussion: interactions between ADV and Profiler

During the steady flow measurements, interactions between ADV and Profiler units were observed when the two units were sampled simultaneously. Their effects in terms data magnitude and quality were tested. Five instrumental setups were experimented under the same flow condition (Q =0.100 m^3/s, d_1 =0.177 m) for the same vertical range (z/d_1 =0.09 to 0.28) (Table 2). The range of vertical elevations was selected based on preliminary measurements during which minimum number of error points was found within the range. In Table 2, y is the transverse distance positive towards the left sidewall. The results showed distinctive interactions between ADV and Profiler units when both instruments were sampled simultaneously. While they did not affect the values of the time-averaged velocity data, the interactions had a significant impact in terms of the velocity fluctuations. The velocity fluctuations at the upper and lower portions of each profile were most adversely affected. The interactions between instruments, including the impact on the data quality, were reduced by rotating the ADV emitter by 180° to face the side wall instead of facing the Profiler control volume, as sketched in Fig. 4B. In the present study, Setups 2 and 3 corresponded to this configuration (Table 2). Further improvements were achieved by moving the ADV longitudinally and transversely away from the Profiler, as in Setup 2. Herein Setups 1 and 2 yielded Profiler data which best compared to the ADV data (Setup 5).

4. Ensemble-averaged measurements and sensitivity analysis

4.1. Presentation

The positive surge propagation was highly repeatable and reproducible in the current setup. The free-surface and velocity characteristics were analysed by repeating the experiment for a number of times and ensemble-averaging the data at a point at an instant ([2],[6]). The synchronisation between different runs for a single flow condition was critical. This was achieved using the ADM sensor located immediately downstream of the gate as a reference (Fig. 4A). When the Tainter gate was closed rapidly, it generated a negative surge propagating downstream, which was characterised by a sudden drop in water elevation, at the same time as the generation of the upstream positive surge. Herein all 50 runs were synchronised based upon the time at which the leading edge of negative surge reached the ADM sensor located downstream of the gate. The ensemble-averaged velocity measurements were performed using Setups 1 and 2 (Fig. 4, Table 2), because they produced the least instrumental interference. The experiments were repeated for a total of 50 runs, 35 run, 25 runs, 15 runs, 10 runs or 5 runs, and the results were ensemble-averaged accordingly.

A number of characteristic unsteady turbulent fluctuating properties were examined: the maximum longitudinal velocity fluctuations occurring shortly after the passage of the bore, the time lag for the maximum longitudinal velocity fluctuation to occur after the bore passage and the longitudinal recirculation velocity (Fig. 7). A definition sketch of the above fluctuating properties is illustrated in Fig. 7, where t is the time since gate closure, t_{bore} denotes the time at which the free-surface started to rise. Mathematically, this time is equal to the instance at which the first derivative of the free-surface elevation with respect to time becomes non-zero. The longitudinal velocity fluctuations were quantified by the difference between the third and first quartile of the total ensemble (V_{75}-V_{25}). The maximum velocity fluctuations $(V_{75}-V_{25})_{max}$ were found to occur shortly after the passage of the bore, and the associated time lag Δt_V was quantified as the delay relative to the time when the free-surface elevation started to rise up. The longitudinal recirculation velocity V_{recirc} marked the minimum velocity reached at the end of the longitudinal deceleration, typically a negative value for the experimental flow conditions. Such a negative

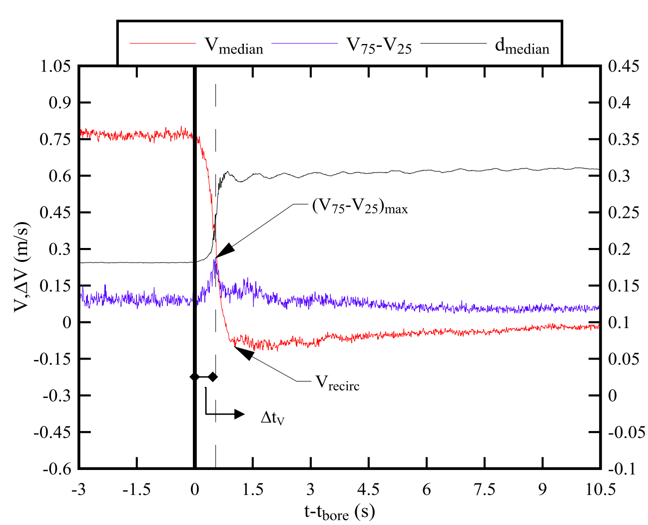

Fig. 7. Instantaneous median water depth, median longitudinal velocity component and longitudinal velocity fluctuation (V_{75}-V_{25}) during a positive surge propagation - Definition sketch of characteristic unsteady turbulent fluctuating properties.

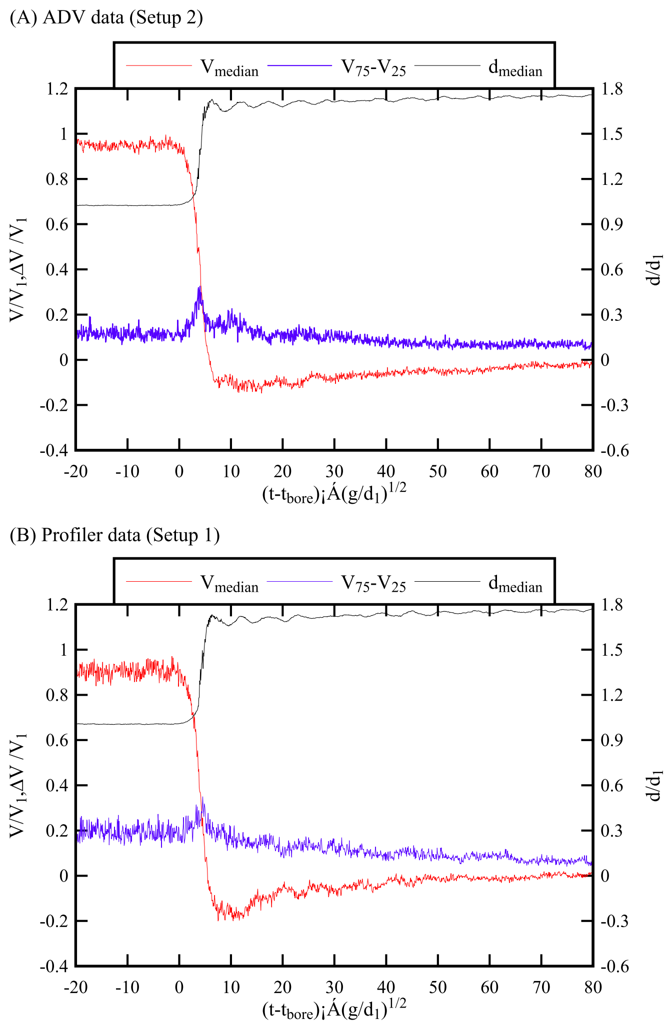

Fig. 8. Ensemble-averaged time-variations of the longitudinal velocity and free-surface elevation at the velocity sampling point during a positive surge: comparison between ADV and Profiler data, both calculated from 50 runs - Flow conditions: $Q = 0.100\ m^3/s$, no radial gate, $h = 0$ m, $z/d_1 = 0.12$. (A) ADV data (Setup 2). (B) Profiler data (Setup 1).

velocity indicated a transient flow reversal and recirculation beneath the surge front. Past and present experimental analysis suggested that the fluctuating properties were characteristics associated with the turbulent nature of the unsteady flow motion [16]. Thus the sensitivity analysis focused on these properties.

4.2. Ensemble-averaged unsteady velocity measurements

Overall, the ensemble-averaged unsteady velocity measurements showed a close agreement between Profiler and ADV velocity data for the same flow conditions and vertical elevation. The passage of the surge was associated with a short and rapid flow deceleration associated with large velocity fluctuations (Figs. 7 and 8). Fig. 8 presents the time-variations of ensemble-averaged longitudinal velocity measured by the ADV (Fig. 8A) and Profiler (Fig. 8B) at the same vertical elevation. The results indicated a close agreement in terms of shape and magnitude of the ensemble-median velocity measured by the two instruments. The velocity fluctuations (V_{75}-V_{25}) obtained with both instruments showed a marked maximum shortly after the passage of the surge front (t-$t_{bore} > 0$). The Profiler data seemed to show a more pronounced recirculation zone in comparison to the ADV data, as highlighted by negative velocity of larger magnitudes at the end of the longitudinal deceleration. Altogether, the time-variations of the unsteady velocity measured by the Profiler, instantaneous or ensemble-average, were very close to those measured by the ADV for all three components. Table 4 compares quantitatively the turbulent fluctuating characteristics measured by Profiler and ADV at similar vertical elevations. The Profiler measurements are presented for two setups, all data being ensemble-averaged over 50 runs. The ADV measurements included present data (Setup 2) ensemble-averaged over 50 runs, and data by [16], ensemble-averaged over 25 runs. The results showed a close agreement between the Profiler data, working alone or with the ADV, and ADV data, working alone or with the Profiler, at a given elevation (Table 4). That is, the Profiler was suitable to conduct high frequency measurements in highly unsteady turbulent flows and captured rapidly fluctuating characteristics with good accuracy, provided that the measurements were taken at vertical elevations where no spurious points existed.

Table 4
Comparison of turbulent fluctuating characteristics in a positive surge between instruments and setups.

Instrument and setup	z/d_1	$(V_{75}$-$V_{25})_{max}$ (m/s) Ensemble-averaged	Δt_V (s) Ensemble-averaged	V_{recirc} (m/s) Ensemble-averaged
Profiler (with ADV) Setup 2	0.13	0.305	0.52	−0.146
ADV Setup 2	0.12	0.263	0.54	−0.119
Profiler alone (Setup 1)	0.13	0.282	0.61	−0.162
ADV alone[a]	0.10	0.215	0.61	−0.239

[a] ADV measurements collected by Leng and Chanson (2016b) at x=8.5 m on channel centreline for the same flow condition. Results were ensemble-averaged over 25 runs.

In the wall region (i.e. $z/\delta < 0.2$, $\rho \times V_* \times z/\mu > 70$), the instantaneous vertical profiles of median longitudinal velocity were tested during the rapid deceleration phase and the early phase after the surge. (Herein the early phase of surge is defined as the period starting immediately after the end of the rapid deceleration phase.). An example is shown in Fig. 9 where the Profiler data are compared to the law of the wall (Eq. (2)). Altogether the data demonstrated that the majority of the data within the wall region compared well to the law of the wall during the rapid deceleration phase, although some scatter was observed. The shear velocity V_* deduced from the best fit of log law was $V_* \approx 0.05$–0.06 m/s for the rapid deceleration, a lower value than the steady flow shear velocity: $V_* = 0.110$ m/s. During the early phase after the surge, the longitudinal velocity profile agrees well with the logarithmic law for

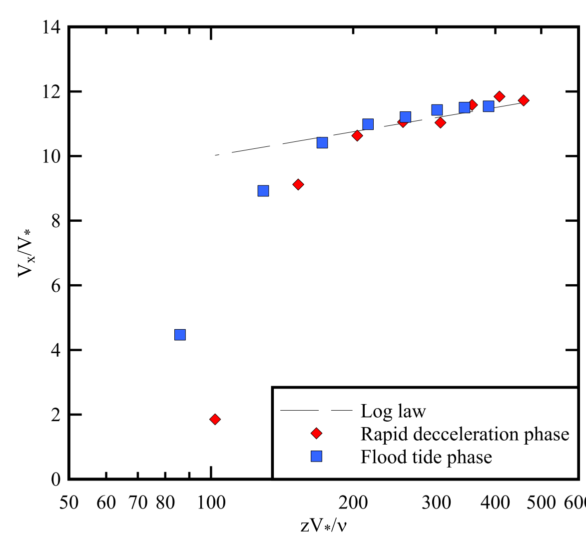

Fig. 9. Vertical distribution of ensemble-averaged median longitudinal velocity in unsteady flow during a positive surge - Comparison between unsteady Profiler data and theoretical logarithmic law (black line) during the rapid deceleration and immediately after the positive surge - Flow conditions: $Q = 0.099\ m^3/s$, $d_1 = 0.097$ m, $Fr_1 = 1.2$.

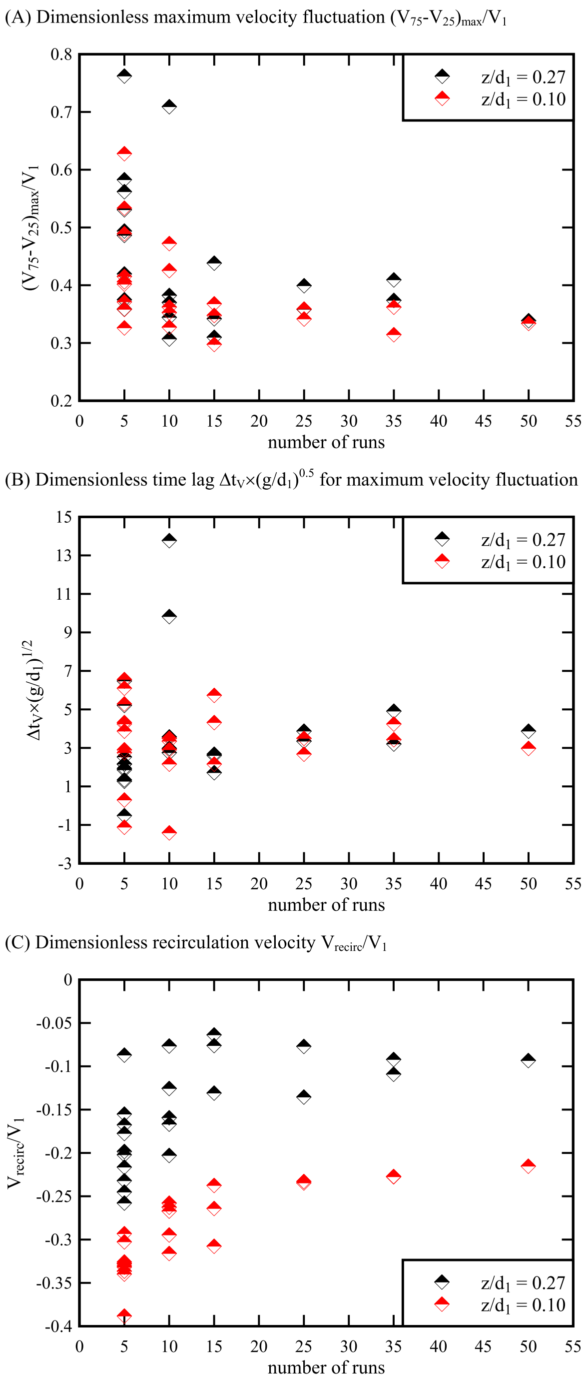

Fig. 10. Sensitivity analysis of characteristic turbulent fluctuating properties in a positive surge at two vertical elevations: ensemble-averaged results as functions of hte number of runs - Profiler sampling alone (Setup 1). (A) Dimensionless maximum velocity fluctuation $(V_{75}\text{-}V_{25})_{max}/V_1$. (B) Dimensionless time lag $\Delta t_V \times (g/d_1)^{0.5}$ for maximum velocity fluctuation. (C) Dimensionless recirculation velocity V_{recirc}/V_1.

the undular bore but not for the breaking bore. A best fit of the law of the wall yielded $V_* \approx 0.05$ m/s (undular surge) and 0.009 m/s (breaking surge) after the surge.

4.3. Sensitivity analysis

The effect of number of experimental repeats runs were analysed in terms of the ensemble-averaged fluctuating characteristics $(V_{75}\text{-}V_{25})_{max}$, Δt_V and V_{recirc}, of the longitudinal velocity data recorded at 7 different vertical elevations: namely, 1 in 5 measuring points out of 35 points in a profile. Fig. 10 presents typical results at two vertical elevations: z/d_1 =0.10 and 0.27. For all flow conditions, the turbulent characteristics showed asymmetrical envelopes of data scatter when the number of runs varied from 50 down to 5. The maximum velocity fluctuations calculated based upon 50 runs tended to be smaller than the average of the results calculated from 35 or 25 runs. The time delay Δt_V obtained from a total ensemble of 50 runs was very close to the average of the time delay obtained from 35 and 25 runs. The magnitude of the recirculation velocity tended to decrease on average as the number of runs increased. The longitudinal deceleration took place in typically less than 0.8 s, a period within which the flow was highly unsteady and intensive turbulent mixing occurred, and the turbulence was likely anisotropic. The time of occurrence of peak velocity fluctuation was different, although only by a few milliseconds during every single run, and the recirculation velocity, defined as the minimum velocity reached at the end of the deceleration phase, occurred at slightly different time as well. Hence, the ensemble-averaging tended to 'smooth' the maximum velocity fluctuation and recirculation velocity over a large number of runs. In practice the number of runs must be large enough to accurately represent the turbulent fluctuating quantities in the rapidly varied flow. Herein 25 and 35 runs were considered most suitable for ensemble-average velocity measurements using the Profiler, with 25 runs being selected as an optimum number of repeats because of time limitations.

5. Conclusion

The acoustic Doppler velocimeter Profiler is a new instrumentation capable of recording up to 35 points quasi-simultaneously at relatively high frequency. But its validation has been limited, mostly to steady flows, and previous studies indicated the existence of outlier data points. Herein new velocity profiling measurements were conducted in steady and unsteady open channel flows at relatively high frequency (100 Hz). The velocity measurements showed a close agreement between the ADV Profiler and traditional ADV data, for the same flow conditions, in terms of the instantaneous median velocity and velocity fluctuations in steady flows, longitudinal velocity recirculation and longitudinal velocity deceleration in positive surges. The instantaneous velocity fluctuations were of the same order of magnitude between Profiler and ADV results. A careful sensitivity analysis was conducted to test the appropriate number of runs for ensemble-averaging in rapidly-varied unsteady flows. The results indicated that the selection of 25 runs was suitable as an optimum number of experimental repeats.

Some instrumental error was observed however with the velocity profiler. Outside of the boundary layer, the Profiler tended to produce errors in terms time-averaged velocity data and velocity fluctuations for a number of points in a profile. Even, at vertical elevations where the time-averaged velocity was meaningful, the vertical distribution of the velocity fluctuations contained errors and erroneous data points.

Overall, the study demonstrated that the propagation of positive surges is a highly unsteady turbulent process, and the performance of ADV Vectrino II Profiler in such an unsteady turbulent flow was satisfactory, provided that a careful validation was undertaken for all Profiler outputs. The velocity profiling may be a valuable technique in unsteady flows, when carefully-controlled experiments can be repeated systematically to ensemble-average the data sets.

Disclosure statement

The authors have no conflict of interest nor any vested interests. This is not an industry sponsored study.

Acknowledgments

The authors thank Professor Pierre Lubin (University of Bordeaux, France) and Dr Hang Wang (The University of Queensland, Australia) for their personal involvement and contribution, as well as Dr Bruce MacVicar (University of Waterloo, Canada), Prof Colin Rennie (University of Ottawa, Canada) and Dr Heide Friedrich (University of Auckland, New Zealand) for helpful comments. The authors acknowledge the technical contribution of Dr Jan Becker (Federal Waterways Engineering and Research Institute, Germany) in the data post-processing program. The authors acknowledge the technical assistance of Jason Van Der Gevel and Stewart Matthews (The University of Queensland). The financial support through the Australian Research Council (Grant DP120100481) is acknowledged.

References

[1] J. Becker. "VTMT (Version 1.1) [Computer software]." Federal Waterways Engineering and Research Institute (BAW), Karlsruhe, 2014. <http://sdrv.ms/12eHgvw/> (accessed on 19 Nov. 2014)
[2] P. Bradshaw, An Introduction to Turbulence and its Measurement, The Commonwealth and International Library of Science and technology Engineering and Liberal Studies, Thermodynamics and Fluid Mechanics Division 218, Pergamon Press, Oxford, UK, 1971 (pages).
[3] H. Chanson, The Hydraulics of Open Channel Flow: An Introduction., 2nd edition, Butterworth-Heinemann, Oxford, UK, 2004, p. 630 (pages).
[4] H. Chanson. Acoustic Doppler Velocimetry (ADV) in the Field and in Laboratory: Practical Experiences. Proceedings of the International Meeting on Measurements and Hydraulics of Sewers IMMHS'08, Summer School GEMCEA/LCPC, 19-21 Aug. 2008, Bouguenais, Frédérique Larrarte and Hubert Chanson Editors., Hydraulic Model Report No. CH70/08, Div. of Civil Engineering, The University of Queensland, Brisbane, Australia, Dec., 2008 pp. 49-66
[5] H. Chanson Applied Hydrodynamics: An Introduction. CRC Press, Taylor & Francis Group, Leiden, The Netherlands, 2014, 448 pages & 21 video movies
[6] H. Chanson, N.J. Docherty, Turbulent velocity measurements in open channel bores, Eur. J. Mech. B/Fluids 32 (2012) 52–58. http://dx.doi.org/10.1016/j.euromechflu.2011.10.001.
[7] H. Chanson, M. Trevethan, C. Koch, Turbulence measurements with acoustic Doppler Velocimeters Discussion, J. Hydraul. Eng., ASCE 133 (11) (2007) 1283–1286. http://dx.doi.org/10.1061/(ASCE)0733-9429(2005)131:12(1062).
[8] R.G.A. Craig, C. Loadman, B. Clement, P.J. Ruesello, E. Siegel. Characterization and Testing of a new Bistatic Profiling Acoustic Doppler Velocimeter: The Vectrino-II. Proc. IEEE/OES/CWTM 10th Working Conference on Current, Waves and Turbulence Measurement (CWTM), Monterey, Canada, 20-23 March, 2011, pp. 246-252 (DOI: 10.1109/CWTM.2011.5759559).
[9] H. Friedrich, S.M. Spiller, N. Rüther. Near-bed flow over a fixed gravel bed. Proc. 7th International Conference on Fluvial Hydraulics (River Flow), Lausanne, Switzerland, 3-5 Sept., 2014, pp. 279-285
[10] D.G. Goring, V.I. Nikora, Despiking Acoustic Doppler Velocimeter Data, J. Hydraul. Eng., ASCE 128 (2002) 117–126.
[11] F.M. Henderson, Open Channel Flow, MacMillan Company, New York, USA, 1966.
[12] H.G. Hornung, C. Willert, S. Turner, The flow field downstream of a hydraulic jump, J. Fluid Mech. 287 (1995) 299–316.
[13] C. Koch, H. Chanson, Turbulence measurements in positive surges and bores, J. Hydraul. Res., IAHR 47 (2009) 29–40. http://dx.doi.org/10.3826/jhr.2009.2954.
[14] X. Leng, H. Chanson, Breaking bore: physical observations of roller characteristics, Mech. Res. Commun. 65 (2015) 24–29. http://dx.doi.org/10.1016/j.mechrescom.2015.02.008.
[15] X. Leng, H. Chanson,. Unsteady Turbulent Velocity Profiling in Open Channel Flows and Tidal Bores using a Vectrino Profiler. Hydraulic Model Report No. CH101/15, School of Civil Engineering, The University of Queensland, Brisbane, Australia, 2016, 118 pages (ISBN 978-1-74272-145-3).
[16] X. Leng, H. Chanson, Coupling between free-surface fluctuations, velocity fluctuations and turbulent Reynolds stresses during the upstream propagation of positive surges, bores and compression waves, Environ. Fluid Mech. 16 (2016) 695–719. http://dx.doi.org/10.1007/s10652-015-9438-8.
[17] J.A. Liggett, Fluid Mechanics, McGraw-Hill, New York, USA, 1994.
[18] J. Lighthill, Waves in Fluids, Cambridge University Press, Cambridge, UK, 1978, p. 504 (pages).
[19] B. Macvicar, S. Dilling, J. Lacey, K. Hipel. A Quality Analysis of the Vectrino II Instrument using a New Open-source MATLAB Toolbox and 2D ARMA Models to Detect and Replace Spikes. Proc. 7th International Conference on Fluvial Hydraulics (River Flow), Lausanne, Switzerland, 3-5 Sept., 2014, pp. 1951-1959
[20] V. Martin, T.S.R. Fisher, R.G. Millar, M.C. Quick. ADV data analysis for turbulent flows: Low correlation problem. Proceedings of Conference on Hydraulic Measurements and Experimental Methods, ASCE-EWRI & IAHR, Reston Va, USA (CD-ROM). 2002
[21] H. Nakagawa, I. Nezu, Prediction of the contributions to the Reynolds stress from bursting events in open-channel flows, J. Fluid Mech. 80 (1977) 99–128.
[22] I. Nezu, Open-Channel Flow Turbulence and its Research prospect in the 21st Century, J. Hydraulic Engineering 131, ASCE, 2005, pp. 229–246.
[23] I. Nezu, W. Rodi, Open-Channel Flow Measurements with a Laser Doppler Anemometer, J. Hydraul. Eng., ASCE 112 (1986) 335–355.
[24] Nortek, Vectrino Profiler: User Guide, Nortek Scientific Acoustic Development Group Inc., User Manual, 2012.
[25] S.B. Pope, Turbulent Flows, Cambridge University Press, 2000, p. 771 (pages).
[26] H. Schlichting, Boundary Layer Theory., 7th edition, *McGraw-Hill*, New York, USA, 1979.
[27] B. Simon, H. Chanson. Turbulence Measurements in Tidal Bore-like Positive Surges over a Rough Bed. Hydraulic Model Report No. CH90/12, School of Civil Engineering, The University of Queensland, Brisbane, Australia, 2013, 176 pages
[28] Q. Xie. Turbulent Flows in Non-Uniform Open Channels: Experimental Measurements and Numerical Modelling. Ph.D. thesis, Dept. of Civil Eng., University Of Queensland, Australia, 1998, 339 pages
[29] H. Wang, L.K. Beckinghma, C.Z. Johnson, U.R. Kiri, H. Chanson. Interactions between Large Boundary Roughness and High Inflow Turbulence in Open channel: a Physical Study into Turbulence Properties to Enhance Upstream Fish Migration. Hydraulic Model Report No. CH103/16, School of Civil Engineering, The University of Queensland, Brisbane, Australia, 2016, 74 pages
[30] L. Zedel, A. Hay. Turbulence Measurements in a Jet: Comparing the Vectrino and Vectrino II. Proc. IEEE/OES/CWTM 10th Working Conference on Current, Waves and Turbulence Measurements (CWTM), Monterey, Canada, 20-23 March, 2011, pp. 173-178 (DOI: 10.1109/CWTM.2011.5759547).

Xianqian Leng is a postgraduate research student at the University of Queensland. Her research interests include experimental investigations of unsteady rapidly-varied open channel flows, computational fluid dynamics (CFD) modelling of bores and positive surges, and field investigations of tidal bores. She authored 18 peer-reviewed papers, including ten international scientific journal articles.

Hubert Chanson is a Professor in Civil Engineering, Hydraulic Engineering and Environmental Fluid Mechanics at the University of Queensland, Australia. His research interests include design of hydraulic structures, experimental investigations of two-phase flows, applied hydrodynamics, hydraulic engineering, water quality modelling, environmental fluid mechanics, estuarine processes and natural resources. His publication record includes over 700 international refereed papers and several books, and his work was cited over 3,200 times (WoS) to 12,500 times (Google Scholar) since 1990. In 2016, his h-index is 29 (WoS), 32 (Scopus) and 54 (Google Scholar).